

# Design of an experimental setup to achieve sinusoidal temperature oscillation in ultrahigh vacuum

F. Pesty<sup>a)</sup> and P. Garoche

*Laboratoire de Physique des Solides, CNRS UMR8502, Université Paris-Sud, Bâtiment 510, 91405 Orsay cedex, France*

(Received 8 August 2002; accepted 2 December 2002)

We designed an experimental setup to produce a temperature oscillation at the surface of a sample, in ultrahigh vacuum. The heating device, a tungsten wire, uses infrared radiation to heat the sample. A regular sine wave cannot produce a harmonic power oscillation, due to the nonlinear character of the Stefan–Boltzmann law of radiation. To achieve it we generate a complex wave form to take into account the thermal behavior of the heating filament as well as its electronic transport properties. An example of temperature oscillation is shown in the case of a tantalum sample, at a 0.12 Hz frequency. It exhibits harmonic behavior with an oscillation amplitude of about 1 K. This method opens the field to new experiments in surface science, to study reversible surface phase transitions.

© 2003 American Institute of Physics. [DOI: 10.1063/1.1544420]

## I. INTRODUCTION

Surface studies lack thermodynamic information, though they present a key interest in many aspects of surfaces, interfaces, or nanostructures physics. This article deals with the possibility of thermal investigations in such fields. These investigations usually consist in bringing an amount of heat to a sample, then examining its response, for instance, its temperature variation. Ac calorimetry measurements to probe thermal properties require sinusoidal temperature oscillation, because it is based on a linearization of the heat diffusion equation.<sup>1–3</sup> This linearization only holds within a narrow frequency range, so the thermal response can only be accurately analyzed if the thermal excitation is purely harmonic. Moreover a sinusoidal excitation allows lock-in detection, and more interestingly provides unique information about the characteristic thermal time constants of the system,<sup>4,5</sup> thanks to the determination of the oscillating response thermal phase shift as a function of frequency. Furthermore, Fourier analysis of the response may provide additional insights on possible nonlinear thermal properties.

In the case of surface studies, requiring ultrahigh vacuum, it is not easy to realize a temperature oscillation and measure it. Several heating methods may be considered: self-heating, resistive, electron bombardment, solid heat conduction, infrared (IR) heating, and laser heating. However, there is a drastic limitation of choice in the case of semiconducting, transparent, or insulating materials: resistive self-heating is not possible, intrinsically, nor electron bombardment, since no bias potential can be applied to the surface. In this article, infrared heating from a local filament has been preferred to laser heating because it provides a wide infrared band, which is appropriate for transparent materials or materials displaying a complex absorption spectrum. It can easily be applied to a wide variety of materials, including insulating ones.

Though the example we discuss concerns a refractory conducting material, tantalum, the method can be used for most other physical systems, in a wide temperature range.

There is a need for periodical excitation, to enable studies of reversible phenomena. In particular, it is possible to separate the reversible part from the irreversible contribution.<sup>6</sup> At the same time, it is necessary to be able to produce harmonic excitation, since in this case the analysis of the response is easy to interpret. Indeed, either the response is harmonic, then we are faced with a linear system, or it leads to second (or higher) harmonic generation, then its measurement provides useful insights about the physics of the phenomena. Of course, in the latter case, we must get rid of inharmonic contributions in the excitation itself, otherwise results are not likely to be easily interpreted.

For this purpose, we propose a thermal model that allows the generation of a pure harmonic temperature oscillation by finding a particular solution to the nonlinear differential equation of the heat exchange in the heating filament, in which both the heat capacity and the electrical resistance have a temperature dependence. Then, we present an experimental example of a harmonic temperature oscillation obtained with this method. Finally, we discuss some applications in the field of surface studies.

## II. PRINCIPLE OF OPERATION

### A. Experimental setup

To obtain a pure sinusoidal temperature oscillation of the sample it is necessary to produce a sinusoidal oscillation of the heating power. This assumes that the sample oscillation range is not too large, so that the sample heat capacity and thermal conductivity (which generally both depend on temperature) can be considered constant within the small temperature excursion. We emphasize that a heating system based on IR radiation is a nonlinear one, because the Stefan–Boltzmann law of radiation is highly nonlinear in temperature. However, as we will see, linear excitation is possible,

<sup>a)</sup>Author to whom correspondence should be addressed; electronic mail: pesty@lps.u-psud.fr

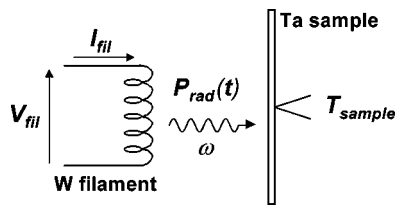


FIG. 1. Schematic of the experimental setup. The sample is a tantalum foil, heated from behind by the radiated power emitted by a heated tungsten filament.  $P_{\text{rad}}$  is converted from the Joule power dissipated within the filament. The temperature is measured with a type K thermocouple welded on the outer side of the foil.

taking into account the variation of some important parameters and finding a periodic, steady-state solution to the differential equation describing the nonlinear thermal process.

Our heating setup is displayed in Fig. 1. It includes a heating filament generating the IR radiation. Located behind the sample, it is made of a long tungsten wire ( $L = 1$  m), 0.1 mm diam. The wire loops are geometrically arranged so that the emitted flow is almost equivalent to a uniformly heated emitting surface. A heating voltage  $V_{\text{fil}}(t)$  is applied between the filament terminals, using a digital wave generator (see Sec. II D). As we will see, the voltage is synthesized with a complex wave form that is numerically computed after solving the thermal equations. It produces the heating current  $I_{\text{fil}}(t)$  of the filament. The Joule power dissipated within the filament is mostly converted into radiation power.

The sample holder is not shown. It allows us to transfer the sample in ultrahigh vacuum (base pressure below  $10^{-9}$  Torr), where *in situ* surface studies are possible, such as low-energy electron diffraction (LEED).<sup>7</sup>

The resulting temperature oscillation is measured with a type K (chromel–alumel) thermocouple welded on the front side of the sample, a 0.2-mm-thick tantalum foil. The oscillation is Fourier analyzed. It must be noted that for small amplitude oscillations—about 1 K—the nonlinear contribution from the type K thermocouple (about  $2 \times 10^{-4}$  K) can be safely neglected.

## B. Nonlinear system

If filament electrical resistance  $R_{\text{fil}}$  was constant along an excitation period, then the Joule power dissipated within the wire would simply follow the same temporal variation than the one of the squared voltage:  $P_{\text{Joule}} = V_{\text{fil}}^2/R_{\text{fil}} \propto V_{\text{fil}}^2(t)$ . In fact, the electrical resistivity of a metal such as tungsten strongly depends on temperature. In our studied temperature range—i.e., between ambient temperature and about 1600 K— $R_{\text{fil}}$  varies almost linearly with the filament temperature,  $T_{\text{fil}}$ . Since the dissipated Joule power is partly used to change  $T_{\text{fil}}$ , the consequence is a time dependence of the filament temperature, and thus the resistance. This means the resistance is not constant along an excitation period, so that the expected behavior of the heating process clearly will not be Ohmic. Let us write the Joule power as  $P_{\text{Joule}} = V_{\text{fil}}(t) \times I_{\text{fil}}(t)$ , and compute the filament resistance as  $R_{\text{fil}}(t) = V_{\text{fil}}(t)/I_{\text{fil}}(t)$ .

Assuming a perfect blackbody radiation, we use the

Stefan–Boltzmann law to write the power radiated by the heated wire:

$$P_{\text{rad}}(t) = \sigma \varepsilon A T_{\text{fil}}^4(t), \quad (1)$$

where  $\sigma = 5.67 \times 10^{-12}$  W K<sup>-4</sup> cm<sup>-2</sup> is the Stefan–Boltzmann constant,  $\varepsilon$  is the emissivity factor, and  $A$  the emitting area of the filament.

Note that the average filament temperature is much higher than the sample temperature: for example, it must be around 1100 K to obtain about 460 K on the sample. This means that the power emitted by the filament is much larger than the power radiated back from the sample to the filament. In first approximation, the latter corresponds to an average power yielding a constant rise in the filament temperature. So, the effect of small sample temperature modulation is completely negligible. Because of the large frequency bandwidth of the energy distribution in a blackbody radiation spectrum (several  $k_B T_{\text{fil}}$ ),<sup>8</sup> we can safely consider the  $\varepsilon$  factor as a constant.

Let us invert Eq. (1) to obtain the time evolution of the filament temperature:

$$T_{\text{fil}}(t) = [P_{\text{rad}}(t)/\sigma \varepsilon A]^{1/4}. \quad (2)$$

Let us now assume in a first step that all the Joule power is converted into radiation power. We will later refine this assumption by taking into account retardation effects due to the finite filament heat capacity. So, energy conservation enables us to write the power balance as  $P_{\text{rad}} = P_{\text{Joule}}$ . The wanted variation for the radiation power can now be expressed as a sinusoidal wave form. This is written:

$$P_{\text{rad}}(t) = P_0 + P_\omega \sin \omega t. \quad (3)$$

We may now evaluate the variation that the filament temperature has to follow by combining Eqs. (2) and (3):  $T_{\text{fil}} \propto (a + b \sin \omega t)^{1/4}$ . This variation is, in turn, used to calculate the optimum wave form for the heating voltage:

$$V_{\text{fil}} = \sqrt{R_{\text{fil}} \times P_{\text{Joule}}} \propto T_{\text{fil}}^{5/2}. \quad (4)$$

This means that we need to produce a heating voltage varying as the 5/8th power of a sine wave:

$$V_{\text{fil}}(t) \propto (c + d \sin \omega t)^{5/8}, \quad (5)$$

where  $c$  and  $d$  are normalization parameters. This formula shows that, though the thermal system is nonlinear, an analytically computable solution can be obtained.

## C. More realistic model

The previous equations would be correct if the filament heater were to respond to the excitation with an infinitely short delay. This cannot occur because the filament has a finite mass, and hence, a finite heat capacity,  $C_p$ . Taking this into account yields a better modeling of the thermal system. The power balance is written now:

$$P_{\text{Joule}} = P_{\text{rad}} + P_{\text{calor}}, \quad (6)$$

where the “calorific power”  $P_{\text{calor}}$  stands for the power that has to be exchanged with the filament to vary its internal energy as the temperature is varied. It is directly proportional to the rate of temperature change:

$$P_{\text{calor}}(t) = C_p \times \frac{dT_{\text{fil}}(t)}{dt}, \quad (7)$$

where the filament heat capacity is the sum of two terms:  $C_p = C_{\text{ph}} + \gamma T_{\text{fil}}$ . The first term is the contribution of lattice vibrations (phonons). In the temperature range of interest it is independent of the temperature, due to the law of Dulong and Petit.<sup>8</sup> In the case of our filament, we estimate<sup>9</sup>  $C_{\text{ph}} \approx 0.027 \text{ J/K}$ . The second term arises from the conduction electron contribution. It gives rise to a linear variation in  $T$ . We estimate it to be:  $\gamma \approx 1.4 \times 10^{-6} \text{ JK}^{-2}$ . It accounts for the (small)  $C_p$  variation along the excitation period, through its dependence in  $T_{\text{fil}}$ .

According to Eq. (7), the calorific power is proportional to the algebraic temperature variation rate,  $dT/dt$ , which means that it can be absorbed or released according to the sign of the rate. The full problem is thus transformed into a nonlinear differential equation in  $T_{\text{fil}}(t)$ :

$$\frac{V_{\text{fil}}^2(t)}{R_1 T_{\text{fil}}(t)} = (\sigma \varepsilon A) T_{\text{fil}}^4(t) + C_p(t) \frac{dT_{\text{fil}}(t)}{dt}, \quad (8)$$

where the  $R_1$  parameter is the resistance linear coefficient. In fact, a more complete description of  $R_{\text{fil}}$  also takes into account smaller terms in a parabolic expansion:

$$R_{\text{fil}}(t) = R_{\text{fil}}[T_{\text{fil}}(t)] = R_0 + R_1 T_{\text{fil}} + R_2 T_{\text{fil}}^2, \quad (9)$$

with  $R_0 = -2.55 \text{ } \Omega$ ,  $R_1 = 0.0276 \text{ } \Omega/\text{K}$ , and  $R_2 = 2.4 \times 10^{-6} \text{ } \Omega/\text{K}^2$ , in the case of our tungsten filament. We use expansion (9) in the following.

The general solution to Eq. (8) is unknown, especially when  $V(t)$  contains trigonometric functions. Since all the terms may be of the same order of magnitude, the usual approximations cannot be made. However, the particular solution as expressed in Eq. (2) can still be tried. Since  $P_{\text{rad}}$  is sought with a sinusoidal variation [Eq. (3)], and since Eq. (1) still holds, an analytical solution is reachable again. In effect, we are looking for a steady-state solution. In particular, the calorific power can be expressed by derivating Eq. (2), to give:

$$\frac{dT_{\text{fil}}}{dt}(t) = (\sigma \varepsilon A)^{-1/4} \frac{d}{dt} (P_{\text{rad}}^{1/4}). \quad (10)$$

So that:

$$P_{\text{calor}}(t) = \frac{C_p(t)}{4} \omega (\sigma \varepsilon A)^{-1/4} P_{\omega}(P_0 + P_{\omega} \sin \omega t)^{-3/4} \cos \omega t. \quad (11)$$

The wave form of the wanted filament voltage can now be written in the following analytic form:

$$V_{\text{fil}}(t) = \sqrt{R_{\text{fil}}(t)} \times \sqrt{P_0 + P_{\omega} \sin \omega t + P_{\text{calor}}(t)}. \quad (12)$$

Note that by assuming  $R_0 = 0$ ,  $R_2 = 0$ , and  $C_p = 0$ , we recover the particular variation in the 5/8th power of a sine wave [Eq. (5)].

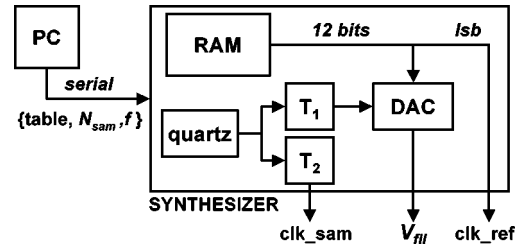


FIG. 2. Schematic of the digital synthesizer. A table of  $N_{\text{sample}}$  11 bit voltage values is computed in the PC, representing the periodical wave form to be applied between the heater terminals. The values are transmitted to the synthesizer using the serial port, and stored in a RAM. A quartz oscillator provides the timing of data conversion, through the digital-to-analog converter (a 12 bit DAC), as well as the timing of data sampling, by synthesizing TTL signals such as “clk\_sam,” generated by the timer  $T_2$ , and “clk\_ref,” built from the least significant bit (lsb) of the digital signal.

### D. Generating the nonharmonic wave form

Since the filament temperature has to follow a periodical variation, so does the voltage applied to the heating filament. The nonharmonic wave form (12) cannot be provided through a conventional sine wave generator, however, it is easily synthesized by digital-to-analog converters. For that purpose we used a digital synthesizer described in Fig. 2.

The wave-form time evolution is obtained by scanning a set of memory addresses, using digital counters— $T_1$  and  $T_2$  in Fig. 2—fed with a single master clock: a 1 MHz quartz oscillator. The computer (PC) calculates the wave form according to Eq. (12), as a table of  $N_{\text{sample}}$  12 bit values. It sends these values to the synthesizer memory (RAM) through its serial port. The values feed the digital-to-analog converter (DAC), at precise times that are computed according to the wanted excitation frequency,  $f_{\text{exc}}$ , at a rate given by timer  $T_1$ .

The very same clock is used to synthesize the excitation wave form (providing  $V_{\text{fil}}$  to the heater) as well as other signals perfectly locked in phase with it: a reference clock, “clk\_ref,” and a sampling clock, “clk\_sam.” These two signals enable the determination of the absolute phase shift and the sampling of physical quantities, for instance, the heating parameters ( $V$  and  $I$ ) and the measured temperature. The clocks can also be used to synchronize a video camera filming the temporal evolution of a low-energy electron diffraction pattern<sup>7</sup> produced by the heated sample. In this article, we focus on the measurement of the thermal evolution of our sample temperature, and on the determination of the thermal behavior of the heating wire itself.

### III. EXPERIMENTAL RESULTS

Our setup enables simultaneous measurement of three parameters: the sample surface temperature,  $T_{\text{sam}}$ ; the effective heating voltage between the two heater terminals,  $V_{\text{fil}}$ ; and the heater current passing through it,  $I_{\text{fil}}$ . Figure 3 displays an experimental result showing the voltage and current evolutions as functions of time, in the unit of phase (degrees) within a single excitation period. The frequency  $f_{\text{exc}}$  is here set to 0.12 Hz. It is low enough to allow good temperature homogeneity within the sample. It is high enough to illustrate the need to take  $P_{\text{calor}}$  into account.

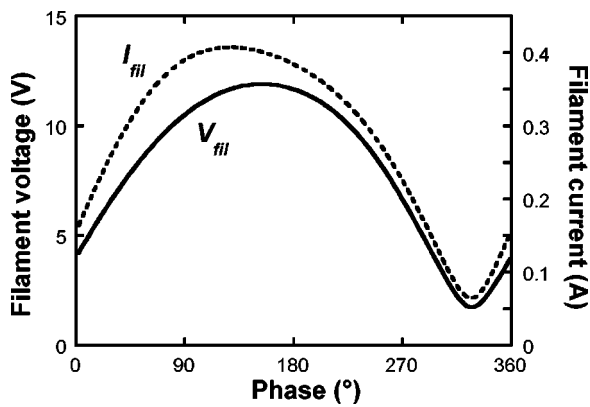


FIG. 3. Experimental filament voltage (solid line) and current (dashed line). Note the non-harmonic-like wave form for both curves, as well as the phase shift between voltage and current, due to the heater resistance time variation. Oscillation frequency is set to 0.12 Hz.

The solid line corresponds to the measured voltage, as applied to the heating wire according to Eq. (12). Its shape is clearly far from a harmonic variation. Because of the need to include a significant  $P_{\text{calor}}$  contribution, it is asymmetric. Due to the time dependence of the filament resistance, the current (dashed line) exhibits non-Ohmic behavior: it is simply not proportional to the voltage.

Measuring these two quantities enables the determination of two instantaneous values:  $P_{\text{Joule}}(t)$ , the dissipated power within the filament, and  $R_{\text{fil}}(t)$ , the filament resistance.  $R_{\text{fil}}$  allows us to compute the instantaneous filament temperature,  $T_{\text{fil}}(t)$ , and thus the radiated power  $P_{\text{rad}}(t)$ , according to Eq. (1). At this step, an adjustable parameter is missing: an estimated product  $\varepsilon \times A$ . It is provided by comparing the measured  $P_{\text{rad}}(t)$  [using Eq. (1)], with the measured difference  $P_{\text{Joule}} - P_{\text{calor}}$ , where  $P_{\text{Joule}}$  is given by the product of the measured filament voltage and current (dark squares), while  $P_{\text{calor}}$  (dark diamonds) is evaluated using Eq. (7). The resulting powers are displayed in Fig. 4 versus the phase within the excitation period.

Note that the sign of  $P_{\text{calor}}$  changes along a period. At

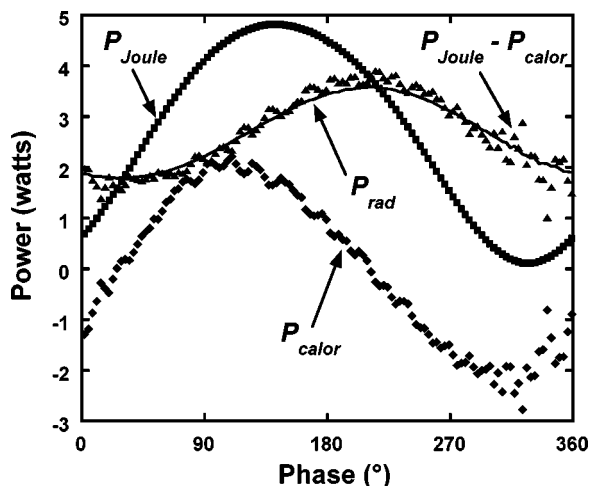


FIG. 4. Time evolution of the radiated power (solid line) is compared with an independent curve (black triangles), plotting the difference between the power dissipated in the filament due to Joule effect (black squares) and the calorific power absorbed or released within the filament (black diamonds).

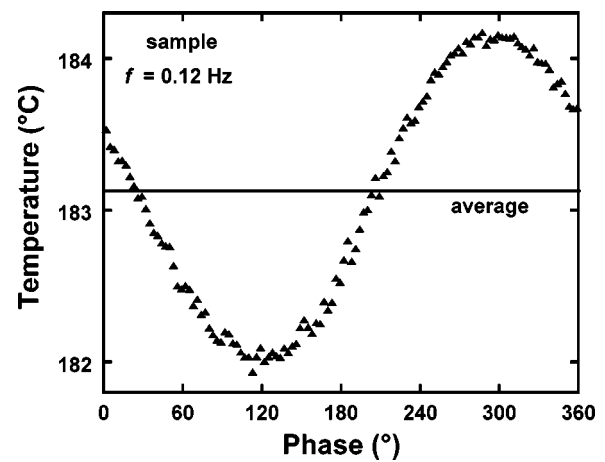


FIG. 5. Resulting time evolution of the sample temperature. The average temperature is about 183.1 °C (456.3 K). The oscillation amplitude at the fundamental frequency is about 1.08 K, with a  $2f$  component of only about 22 mK. Note the offset of the temperature axis.

this frequency,  $P_{\text{calor}}$  and  $P_{\text{Joule}}$  are of comparable magnitudes. By the difference between the two quantities (dark triangles), a best fit to the determined  $P_{\text{rad}}$  is obtained (solid line) choosing a value  $\varepsilon \times A \approx 0.3 \text{ cm}^2$ . This adjustable parameter acts on the vertical position of the  $P_{\text{rad}}$  vs phase curve, while the  $C_p$  parameter mainly acts on the horizontal position of the  $P_{\text{Joule}} - P_{\text{calor}}$  curve. The  $C_p$  value computed from the evaluated filament mass accounts well for the observed behavior (within a few %). Note the large phase shift between the radiated power and the Joule power.

The good agreement between the curves obtained by these two independent ways validates *a posteriori* our thermal model presented in Sec. II C. Equation (11) means that the finite filament heat capacity is of increasing importance as the working frequency is raised. The example in Figs. 3–5, however, demonstrates that a fairly high variation rate can nonetheless be achieved with a heating wire characterized by response times of a few seconds. At the working frequency of Figs. 3–5, the filament temperature oscillates between 1012 and 1205 K, which is a moderate excursion. It can rise higher as the frequency is decreased.

This method enables us to tune two independent parameters: the temperature oscillation amplitude and its frequency, through the experimental parameters:  $P_\omega$ ,  $P_0$ , and  $f_{\text{exc}}$  [Eq. (3)]. Figure 5 presents the corresponding temperature oscillation as measured at the sample surface. The average sample temperature is about 183.1 °C. Note the phase shift between the temperature oscillation and the radiated power (respectively, 155.3° and 240.5° in this example), both different from the Joule power phase shift (the phase reference). This is due to different time constants: the filament retardation comes from a finite response time in the filament thermalization, whereas the sample oscillation phase shift with respect to the latter depends on the (rather large) sample heat capacity. The second-harmonic content of the thermal flow can be estimated from the filament temperature, using Eq. (1). Whereas it is about 12.5% with a pure sinusoidal voltage, it is reduced to 2% by adjusting the wave form using Eq. (12).

Also note that the  $2f$  harmonic of the sample temperature oscillation can be very small. In Fig. 5, it represents about 22 mK while the fundamental component oscillation amplitude at  $f$  is slightly higher than 1 K.

The simplified model may be used for very low frequencies (e.g., 0.02 Hz). In this case the filament heat capacity contribution may be fully neglected, and the simpler universal wave form (5) may be used instead of Eq. (12). By varying the frequency and the power parameters, we have been able to produce temperature amplitudes ranging between, typically, 0.005 and 2 K, with a small inharmonic contribution.

#### IV. APPLICATIONS

Several physical applications of our thermal setup may be thought of, most of them related to thermodynamics investigations. Besides the above-mentioned oscillating mode calorimetry,<sup>1</sup> a temperature oscillation may be used to determine the thermal diffusivity of a material.<sup>10</sup> One other important application consists in studying the thermodynamic behavior of a surface in response to thermal excitation. We developed our experimental setup to work in ultra-high-vacuum conditions for the sake of studying thermodynamic behaviors occurring at *surfaces*.

In this respect, we propose to apply the temperature oscillation to a sample, the surface of which is being bombarded with a low-energy electron beam. The resulting diffraction pattern can be measured, and the oscillatory part of the pattern can be recorded using our previously reported oscillating LEED method.<sup>7</sup> If at some critical temperature a

phase transformation occurs at the surface, leading to atomic motions with a signature in the diffraction spots, then a periodic motion of some spots is expected. If the transformation is *reversible*, then an oscillation in the surface temperature must be reflected in an oscillation in the spot positions within the pattern. Elsewhere, we report a preliminary result where such an oscillatory spot motion is recorded with this method.<sup>11</sup> One advantage of the oscillating method, as previously emphasized, lies in the possibility of varying the excitation frequency and determining the phase shift of the response. This makes our method able to give access to response times of the studied physical phenomena.

#### ACKNOWLEDGMENTS

The authors thank S. Senoussi and I. Saillot for careful reading of this manuscript.

<sup>1</sup>G. R. Stewart, Rev. Sci. Instrum. **54**, 1 (1983).

<sup>2</sup>P. F. Sullivan and G. Seidel, Phys. Rev. **173**, 679 (1968).

<sup>3</sup>P. Manuel and J. J. Veyssié, Rev. Gen. Therm. **15**, 231 (1976).

<sup>4</sup>P. Garoche, P. Manuel, and J. J. Veyssié, J. Low Temp. Phys. **30**, 323 (1978).

<sup>5</sup>F. Pesty, P. Garoche, and M. Héritier, Mater. Res. Soc. Symp. Proc. **173**, 205 (1990).

<sup>6</sup>F. Pesty, K. Wang, and P. Garoche, Synth. Met. **27**, B137 (1988).

<sup>7</sup>S. Dorel, F. Pesty, and P. Garoche, Surf. Sci. **446**, 294 (2000).

<sup>8</sup>F. Reif, *Fundamentals of Statistical and Thermal Physics* (McGraw-Hill, Tokyo, 1981), p. 254.

<sup>9</sup>Filament mass of about 0.2 g and a tungsten specific heat  $C_{ph} = 133 \text{ J kg}^{-1} \text{ K}^{-1}$ .

<sup>10</sup>L. Verdini and A. Santucci, Nuovo Cimento Soc. Ital. Fis., B **62**, 399 (1981).

<sup>11</sup>F. Pesty (unpublished).